JACS
JOURNAL OF THE AMERICAN CHEMICAL SOCIETY
pubs.acs.org/JACS
Article

Elusive Protein−Glycosphingolipid Interactions Revealed by Membrane Anchor-Assisted Native Mass Spectrometry

James W. Favell, Duong T. Bui, Jianing Li, Ling Han, Elena N. Kitova, Edward N. Schmidt, Raelynn Brassard, Pavel I. Kitov, Yves St-Pierre, Lara K. Mahal, M. Joanne Lemieux, Matthew S. Macauley, and John S. Klassen*

Cite This: https://doi.org/10.1021/jacs.4c05805

ABSTRACT: Interactions between glycan-binding proteins (GBPs) and glycosphingolipids (GSLs) present in cell membranes are implicated in a wide range of biological processes. However, studying GSL binding is hindered by the paucity of purified GSLs and the weak affinities typical of monovalent GBP−GSL interactions. Native mass spectrometry (nMS) performed using soluble model membranes is a promising approach for the discovery of GBP ligands, but the detection of weak interactions remains challenging. The present work introduces **ME**mbrane **AN**chor-assisted nMS (MEAN-nMS) for the detection of low-affinity GBP−GSL complexes. The assay utilizes a membrane anchor, produced by covalent cross-linking of the GBP and a lipid in the membrane, to localize the GBP on the surface and promote GSL binding. Ligands are identified by nMS detection of intact GBP−GSL complexes (MEAN-nMS) or using a catch-and-release (CaR) strategy, wherein GSLs are released from GBP−GSL complexes upon collisional activation and detected (MEAN-CaR-nMS). To establish reliability, a library of purified gangliosides incorporated into nanodiscs was screened against human immune lectins, and the results compared with affinities of the corresponding ganglioside oligosaccharides. Without a membrane anchor, nMS analysis yielded predominantly false negatives. In contrast, all ligands were identified by MEAN-(CaR)-nMS, with no false positives. To highlight the potential of MEAN-CaR-nMS for ligand discovery, a natural library of GSLs was incorporated into nanodiscs and screened against human and viral proteins to uncover elusive ligands. Finally, nMS-based detection of GSL ligands directly from cells is demonstrated. This breakthrough paves the way for shotgun glycomics screening using intact cells.

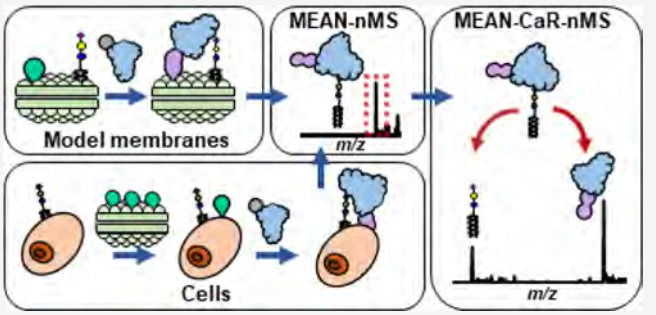

INTRODUCTION

Interactions between membrane-bound glycosphingolipids (GSLs) and glycan-binding proteins (GBPs) are critical to many cellular processes, including cell recognition, signaling and immune responses, and are implicated in a variety of pathophysiological processes, such as cancer progression, neurodegeneration, and bacterial and viral infections.[1−3] Identifying these interactions and elucidating their biological roles may help improve human health by guiding the development of new diagnostics and therapeutics for diseases.[3,4] However, the full repertoire of cellular GSLs recognized by most GBPs has yet to be elucidated.[5−7] Among the key challenges hindering the discovery and characterization of GSL ligands are the limited availability in purified form, their low affinities, and the influence of the lipid (membrane) environment on binding.[7,8] There are ∼378 unique mammalian GSL structures (not including variations in the ceramide moiety) identified to date, but only ∼15 are available commercially in purified form.[9,10] The low affinities (K_d ∼mM) typical of monovalent GBP−GSL interactions make them difficult to detect using most established assays.[6,11] Moreover, while the carbohydrate moiety of GSLs is predominantly responsible for recognition by GBPs, membrane composition, including the nature and concentration of GSLs, affects binding.[12] Consequently, GSL binding studies must be performed using model lipid membranes, such as supported lipid bilayers, mono- and bilayer vesicles, bilayer islands and liposomal nanoparticles, which serve to mimic the natural cell membrane environment.[13,14]

There are a number of analytical assays that are compatible with model membranes and capable of detecting GBP−GSL binding in a way that estimates the corresponding kinetic and thermodynamic parameters. For example, surface plasmon

Received: April 27, 2024
Revised: June 17, 2024
Accepted: July 12, 2024

resonance spectroscopy, fluorescence microscopy and quartz crystal microbalance measurements can be carried out using supported or nanocube lipid bilayers or bilayer islands.[15−20] None of these approaches, however, can directly establish the identity and number of GSL ligands bound to the GBP. Moreover, these methods, which are restricted in their applicability to defined mixtures of purified GSLs and cannot be applied to the analysis of natural GSL libraries extracted from cells or tissue, are of limited utility for ligand discovery. Instead, GSL ligand discovery relies predominantly on microarray-based shotgun glycomics screening, which utilizes a microarray constructed from fluorescently labeled derivatives of fractionated GSLs derived from natural sources (e.g., cells, tissue or biofluids).[7] The microarray approach, however, is limited by the modifications made to the GSLs, their nonnative (membrane-free) presentation, lack of mobility on the surface, and a general inability to detect low-affinity interactions.[21] Moreover, as the modified GSLs are spatially separated on the array, low-affinity ligands that could contribute to cellular recognition through homo- and heteromultivalent binding may go undetected.[18,19,22] Given the limitations in existing assays for the discovery of biologically relevant GSL−GBP interactions, advancing this important area of functional glycomics critically depends on the development of new analytical methods.

Native mass spectrometry (nMS)—which typically involves electrospray ionization (ESI)-mass spectrometry (MS) analysis performed using native-like solution conditions and instrumental parameters that preserve noncovalent complexes—is routinely used to detect and quantify GBP−glycan binding in vitro.[23,24] When implemented with GSLs incorporated into water-soluble bilayer islands, such as nanodiscs (NDs) and picodiscs, nMS has shown promise for the discovery and characterization of GBP−GSL interactions.[11,25−29] To perform these measurements, GSL-containing model membranes are incubated with the target GBP and the mixture analyzed by nMS.[11,25−29] During desolvation, intact GBP−GSL complexes spontaneously dissociate from the model membrane in a process believed to be driven by Coulombic repulsion between the multiply charged GBP and membrane.[11] In some cases, the GSL ligands can be identified directly from the molecular weights (MWs) of the gaseous GBP−GSL complex ions. However, for large or heterogeneous GBPs or for GBPs with multiple binding sites, which can bind to different GSLs, the catch-and-release (CaR)-nMS approach is used, wherein the bound (caught) GSLs are released as ions from the gaseous GBP−GSL complexes by collision-induced dissociation (CID).[11,27] The released GSLs are identified by their MW and, if required, from the diagnostic fragment ions produced by CID.[11,27]

An attractive feature of nMS (and CaR-nMS) for analyzing GBP−GSL interactions is its amenability to model membranes containing mixtures of GSLs extracted from cells or tissue, which is ideal for ligand discovery.[27] However, the detection of low-affinity ligands is challenging, particularly for monovalent GBPs.[23,30−32] In principle, the detection of weak interactions can be enhanced by increasing the GSL concentration.[30] But, bilayer islands tend to be unstable at high GSL content and disassemble, while high concentrations of model membrane lead to ion suppression effects.[33,34]

Here, we introduce the **ME**mbrane **AN**chor-assisted nMS (MEAN-nMS) assay, which enables the detection of low-affinity interactions between soluble GBPs and GSLs in model membranes. The method, inspired by recent findings that high-affinity GSL ligands enhance GBP binding to low-affinity ligands in NDs,[22] relies on the cross-linking of the GBP to the membrane through a modified lipid via a copper-free click reaction. The resulting membrane anchor serves to localize the GBP on the surface of the membrane, which promotes binding by effectively increasing the concentration of GSL in the vicinity of the GBP. A notable feature of MEAN-nMS is that it can be applied to any GBP, including those with a single binding site. We first establish the reliability of MEAN-nMS by screening a library of purified gangliosides incorporated into NDs against human immune lectins and comparing the results with affinities of corresponding ganglioside oligosaccharides. We then demonstrate the potential of MEAN-nMS implemented using CaR (MEAN-CaR-nMS) for discovery by screening NDs containing natural libraries of GSLs extracted from cells against human and viral proteins to uncover elusive GSL ligands. Finally, using MEAN-CaR-nMS, we present the first examples of GSL ligand discovery directly from intact cells.

MATERIALS AND METHODS

Proteins, Lipids, GSLs. Details of the proteins, lipids, GSLs, oligosaccharides and other reagents used in this study are given as Supporting Information, with structures shown in Figure S1.

Cell Culture. Human embryonic kidney 293T (HEK 293T) cells were cultured in Dulbecco's modified Eagle medium/nutrient mixture (Gibco Scientific) containing 10% fetal bovine serum (Gibco), 100 U mL^{-1} penicillin (Gibco), 100 μg mL^{-1} streptomycin (Gibco) and 5 μg mL^{-1} blasticidin (InvivoGen). Human neuroblastoma SH-SY5Y cells were cultured in Eagle's minimum essential media containing 10% fetal bovine serum, 1% penicillin, and 1% streptomycin. All cells were maintained in a 5% CO_2 incubator at 37 °C.

Cell Imaging. Optical and scanning electron microscope imaging was performed on aliquots of HEK 293T cells resuspended in 1× PBS (pH 7.4) or 200 mM ammonium acetate (pH 7.4) before and after sonication (30 min) at room temperature. Details are provided as Supporting Information.

Preparation of NDs. Complete details on ND preparation are provided as Supporting Information.

Membrane Anchor Formation. The copper-free click chemistry reaction, used to form the membrane anchor, was carried out by labeling the GBP with DBCO-PEG_4-NHS ester (details given as Supporting Information and in Figure S2a), and subsequently incubating the DBCO-labeled GBP with azidoPE-ND or GSL-containing azidoPE-ND for 1 h at 25 °C (Figure S2b). For application of MEAN-CaR-nMS directly to cells, azidoPE-ND was mixed with the cells and sonicated for 30 min at room temperature.

Mass Spectrometry. The nMS measurements were performed using a Q Exactive Hybrid Quadrupole Orbitrap mass spectrometer (Thermo Fisher Scientific, Waltham, USA), an ultrahigh mass range Q Exactive Hybrid Quadrupole Orbitrap mass spectrometer (Thermo Fisher Scientific, Waltham, USA) and a Synapt G2S ESI quadrupole-ion mobility separation-time-of-flight mass spectrometer (Waters, Manchester, UK). Each instrument was equipped with a nanoflow ESI source. A description of experimental conditions and instrumental parameters is provided as Supporting Information.

Cell Glycolipid Analysis. GSLs were extracted from HEK 293T and from human neuroblastoma SH-SY5Y cells using the procedure described elsewhere.[35] Briefly, approximately 10×10^6 cells were resuspended in 2 mL ice−cold water and homogenized on ice in a 15 mL tube using an ultrasonic homogenizer. 5.34 mL of methanol was added, followed by 2.67 mL of chloroform. This solution was mixed thoroughly before centrifugation at 4000g for 15 min. The supernatant (containing the GSLs) was carefully decanted into another 15 mL tube, where it was dried under nitrogen gas. A

https://doi.org/10.1021/jacs.4c05805
J. Am. Chem. Soc. XXXX, XXX, XXX−XXX

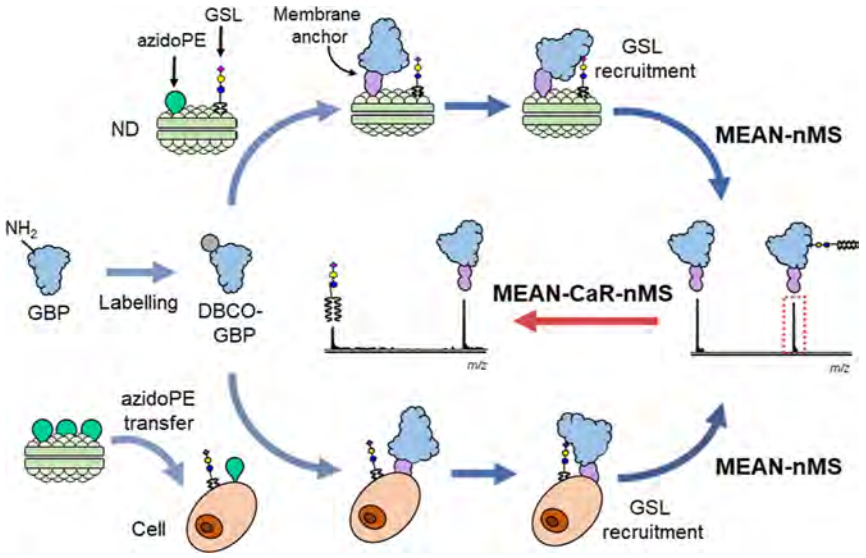

Figure 1. Schematic overview of the MEAN-(CaR)-nMS assay for detecting interactions between GBPs and GSLs present in NDs and cells. The DBCO-labeled GBP is incubated with NDs (containing phospholipid, GSL and azidoPE) or azidoPE-treated (delivered, for example, using azidoPE-NDs) cells. The formation of one or more "membrane anchor" via a copper-free click reaction localizes the GBP on the surface of the membrane and allows for the recruitment of GSL ligands present in the model or cell membrane. The identities of GSL ligands bound to GBP are determined by nMS analysis (from accurate MW measurements of the resulting GBP−GSL complexes) or CaR-nMS analysis [by activating the complexes using CID to release the GSLs (as ions) and identifying them from their MWs].

description of experimental conditions and instrumental parameters is provided as Supporting Information.

Quantifying GSL_{os} Affinities. nMS was used to quantify the GSL oligosaccharide (GSL_{os}) affinities for GBPs. Details of the binding assay and data analysis procedures are provided as Supporting Information.

Quantifying GSL Binding. nMS analysis was used to quantify the fraction of GBP (labeled or unlabeled) bound to GSLs. Details of the data analysis procedures are given as Supporting Information.

RESULTS AND DISCUSSION

Validation of the MEAN-nMS Assay. *Assay Overview.* A schematic overview of the implementation of MEAN-(CaR)-nMS for the detection of GSL ligands in NDs and cells is given in Figure 1. Briefly, the GBP is first labeled with DBCO groups (Figure S2a).[36] It is challenging to precisely control the degree of DBCO labeling due to the instability of the active ester groups, which are susceptible to hydrolysis, and variations in labeling efficiencies.[37,38] However, a 1 h incubation time and 20:1 molar DBCO-PEG_4-NHS/GBP ratio is generally sufficient to achieve >1 DBCO labels. For the applications of MEAN-(CaR)-nMS to NDs, the DBCO-labeled GBP is incubated with NDs containing azidoPE and GSL. The copper-free click reaction (Figure S2b) forms covalent bonds (membrane anchors) between the DBCO and azidoPE (Figure S2b), resulting in ND-associated GBP {referred to here as [GBP + *j*(DBCO−PE)]}. Anchoring the GBP on the ND surface results in an increase in the effective concentration of GSL in the vicinity of the GBP, which promotes binding. During the ESI process, GSL-bound GBP complexes [GBP + *j*(DBCO−PE) + GSL] dissociate from the membrane due to Coulombic repulsion (between the multiply charged GBPs and the ND) and are detected by MS.[11,39] Alternatively, with MEAN-CaR-nMS, the [GBP + *j*(DBCO−PE) + GSL] complex is isolated and subjected to CID and the released GSL ions detected by MS. To apply MEAN-(CaR)-nMS to cells, a suspension of cells is treated with azidoPE-containing ND and the mixture is sonicated to disrupt the cell membrane and facilitate incorporation of azidoPE. The DBCO-labeled GBP is then added, and the mixture analyzed by nMS or CaR-nMS to identify GSL ligands.

GAL-3C and GAL-7. To demonstrate the reliability of MEAN-nMS for detecting GSL ligands in model membranes, eight purified gangliosides (GM1, GM2, GM3, GD1a, GD1b, GD2, GT1a and GT1b) were incorporated, separately, into azidoPE-containing NDs and screened against both unlabeled and DBCO-labeled human galectin-7 (GAL-7) and C-terminal carbohydrate recognition domain of human galectin-3 (GAL-3C). Galectins, which represent an important class of immune lectins, recognize glycans possessing terminal β-galactose (Gal) residues.[40] The GSL specificities of human galectins are not well characterized, although GAL-3C (and GAL-3) and GAL-7 are known to recognize neutral GSLs, including lacto- and neolacto-GSLs.[41−45] Gangliosides are also suggested to bind and there is evidence of GAL-3 and GAL-7 interactions with GM1 on model and cell membranes.[41−45] As the ganglioside binding properties of GAL-3C and GAL-7 have not been comprehensively established, the MEAN-nMS data were assessed by comparison to the affinities (Table S1) of the corresponding ganglioside oligosaccharides measured in the present study (Figures S3 and S4) and previously reported data (for $GM3_{os}$).[46] According to the affinity data, neither $GM2_{os}$ nor $GD2_{os}$ (both of which lack terminal Gal) is recognized by GAL-3C or GAL-7, in line with expectations. The other oligosaccharides tested are all low-affinity ligands, with K_d ranging from 0.2 to 1.5 mM (GAL-3C) and 0.6 to 4 mM (GAL-7), with $GM3_{os}$ being the highest affinity ligand for both GBPs.

For unlabeled GAL-3C, nMS analysis produced weak signals corresponding to the association of GM3, GD1a, GD1b, GT1a and GT1b; no binding to GM1 (false negative), GM2, or GD2 was detected (Figure S5). For unlabeled GAL-7, no binding was observed for any of the gangliosides (Figure S6). Using DBCO-labeled GAL-3C, MEAN-nMS detected ions corresponding to GAL-3C with membrane anchor, as well as 1:1

https://doi.org/10.1021/jacs.4c05805
J. Am. Chem. Soc. XXXX, XXX, XXX−XXX

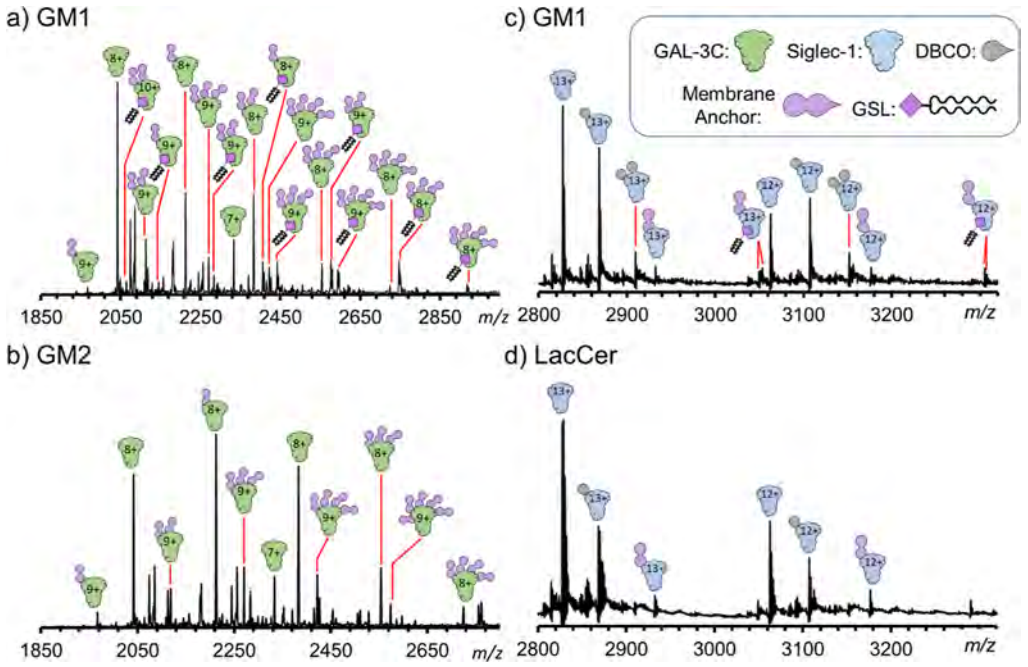

Figure 2. Validation of MEAN-nMS for detecting GSL ligands in NDs. Results from MEAN-nMS analysis performed in positive ion mode on aqueous ammonium acetate solutions (200 mM, 25 °C, and pH 6.8) of DBCO-labeled GAL-3C (3 μM) with 20% azidoPE-ND (10 μM) containing 10% (a) GM1 and (b) GM2; and DBCO-labeled Siglec-1 fragment (3 μM) with 20% azidoPE-ND (10 μM) containing 10% (c) GM1 and (d) LacCer.

complexes with GM1, GM3, GD1a, GD1b, GT1a, and GT1b; no binding to GM2 or GD2 was observed (Figures 2a,b and S7). These results fully align with the measured ganglioside oligosaccharide affinity data (Table S1). The GAL-7 homodimer possessing membrane anchor was also found to bind GM1, GM3, GD1a, GD1b, GT1a and GT1b; no interactions with GM2 and GD2 were detected (Figure S8). These results are also consistent with the oligosaccharide affinities. Despite having two equivalent binding sites, only the 1:1 complexes were detected for GAL-7, suggesting that conformational restrictions resulting from the membrane anchor prevent the homodimer from engaging in multivalent binding. Nevertheless, the membrane anchor did not significantly disrupt the GAL-7 dimer,[47] as judged by the low abundance of detected monomer.

To establish whether the aforementioned GSL binding detected with MEAN-nMS originates from the same ND to which the GBP is anchored, measurements were performed on DBCO-labeled GAL-3C and a mixture of two ND samples—GM3-ND (no azidoPE) and 20% azidoPE ND (no GM3). Notably, no binding between the GAL-3C with membrane anchor and GM3 was detected (data not shown). This finding suggests that, under these conditions, the GSL ligands detected by MEAN-nMS are the result of cis-interactions (between the GBP and GSL in the same ND), with no appreciable contribution from trans-interactions involving GBP and GSL in different NDs.

The ganglioside binding data acquired for GAL-3C and GAL-7 demonstrate how the introduction of a membrane anchor dramatically improves nMS detection of GBP interactions with GSLs. For both proteins, the MEAN-nMS assay detected binding to all six gangliosides possessing a terminal or otherwise accessible Gal residue. Of these, only GM1 has previously been shown to be a ligand.[41−45] That no binding was detected for GM2 and GD2, which lack terminal Gal, establishes that anchoring the GBPs to the ND does not lead to false positives (nonspecific binding). These results are in sharp contrast to the complete absence of detectable binding in the case of unlabeled GAL-7 and the much lower levels of specific binding and false negatives measured for unlabeled GAL-3C. The performance gains achieved with MEAN-nMS are depicted quantitatively in Figure 3, wherein the fraction (F_{GSL}) of GSL-bound GBP is plotted for labeled and unlabeled GAL-3C (Figure 3a) and GAL-7 (Figure 3b) and each ganglioside tested. In the case of GAL-3C, for which five ligands were detected using unlabeled protein, the increase in F_{GSL} ranges from 4- to 20-fold. In the case of the false negatives, the increase in F_{GSL} cannot be quantified as only MEAN-nMS enabled detection of the ligands. It is also instructive to compare the F_{GSL} to values expected for the ganglioside oligosaccharides calculated from the measured K_d (Table S1) at the same concentration as the gangliosides (Figure 3a,b). This analysis shows that, in the absence of a membrane anchor, the extent of GSL binding falls well short of what is expected for the corresponding oligosaccharides. In contrast, the presence of the membrane anchor leads to binding that exceeds that expected for the oligosaccharides.

The greater sensitivity of MEAN-nMS, compared to conventional nMS, for detecting GBP−GSL interactions in NDs is attributed to the higher local concentration of GSL in the vicinity of the GBP when attached to ND via the membrane anchor. From the equilibrium expression ($[GSL]/K_{d,GSL} = [GBP + GSL]/[GBP]$) and assuming that the K_d of the labeled and unlabeled GBP are similar, the concentration ratio (R_{GSL}, eq S11c) of GSL-bound to free GBP is expected to vary linearly with GSL concentration. The increase in effective concentration resulting from sequestration of the GBP on the surface of the ND can be estimated from the ratio of total solution volume-to-total volume occupied by the GBP-bound ND and the concentrations used. Treating the NDs as

https://doi.org/10.1021/jacs.4c05805
J. Am. Chem. Soc. XXXX, XXX, XXX−XXX

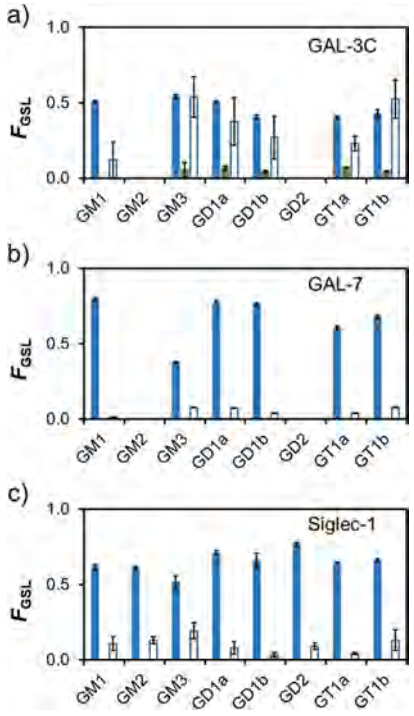

Figure 3. Enhanced detection of GBP binding to GSLs in NDs using MEAN-nMS. Fraction (F_{GSL}) of GSL-bound GBP determined by nMS and MEAN-nMS analysis of aqueous ammonium acetate solutions (200 mM, 25 °C, and pH 6.8) of unlabeled (green bars) and DBCO-labeled (blue bars) (a) GAL-3C, (b) GAL-7 and (c) Siglec-1 fragment, with 20% azidoPE-ND (10 μM) containing 10% GSL (GM1, GM2, GM3, GD1a, GD1b, GD2, GT1a, GT1b or LacCer). Expected F_{GSL} values (white bars) calculated from the K_d measured for the corresponding GSL oligosaccharides. Errors correspond to one standard deviation.

cylinders,[48] the concentration of GSL in the vicinity of the NDs is estimated to be ~1500-fold greater compared to bulk solution (details given as Supporting Information and in Figure S9). Because the volume of the GBP-bound ND is expected to increase with size of anchored GBP, the increase in GSL concentration may be somewhat smaller, although still significant. For example, in the case of GAL-3C and GAL-7, the increase in effective GSL concentration is estimated to be approximately 160- to 1000-fold. Based on these concentration increases, F_{GSL} is expected to increase 10- to 20-fold, which is in line with the experimental observations. It should be noted, though, that the F_{GSL} values measured with MEAN-nMS may also be influenced by other factors. In particular, the presence of the membrane anchor is expected to result in unbound and GSL-bound GBP ions having similar nMS response factors. In contrast, for unlabeled GBP, the free and GSL-bound ions will exhibit nonuniform response factors (the free GBP ions are transferred directly to the gas phase, while the GSL-bound GBP ions are initially associated with the ND), which will affect their relative abundances in the gas phase.[39]

Discovery of GSL Ligands by MEAN-(CaR)-nMS. The results obtained for GAL-3C and GAL-7 highlight the advantage of a membrane anchor for detecting binding between soluble GBP and GSLs in model membranes by nMS. To further showcase the utility of this strategy for ligand discovery, the MEAN-(CaR)-nMS approach was used to probe the ganglioside binding properties of the human immune lectin Siglec-1 and the receptor-binding domain (RBD) of SARS-CoV-2.

Siglec-1. Siglec-1, also known as sialoadhesin or CD169, is a member of the sialic acid-binding immunoglobulin-type lectins (Siglecs), which are found primarily on the surface of immune cells.[49,50] They serve important roles in immune system regulation and intracellular and intercellular signaling and are associated with the development of diseases, including autoimmune diseases, neurodegenerative conditions, and cancer.[49−53] Siglec functions are regulated through binding to sialic acid (Sia)-containing glycans (sialoglycans) conjugated to proteins and lipids.[49−53] Unlike other Siglecs, Siglec-1, which is expressed on the surfaces of macrophages and dendritic cells, possesses no inhibitory motifs, instead serving in an activatory role, enhancing phagocytosis by binding sialoglycans located on cells, extracellular glycolipids and glycoproteins, or pathogens.[50,53] It has been shown that Siglec-1 preferentially recognizes α2-3-linked Sia, followed by α2-6-, and α2-8-linked Sia.[49,50,54] However, due to their low affinity, the glycan-binding specificities of Siglec-1 have not been fully established.[14,49,52,53]

Recently, the specificities of human Siglecs 1-11 and -15 for gangliosides were profiled using four different assays.[55] Binding data for a soluble dimeric Siglec-1-Fc fusion complexed with tetrameric Strep-Tactin horseradish peroxidase conjugate measured with a lipid bilayer-free ELISA suggested that all nine gangliosides tested (GM1, GM2, GD1a, GD1b, GD3, GT1b, GM3, GM4 and GQ1b) are ligands, with GM2 and GM3 exhibiting the strongest avidities.[55] Using 3 mol % glycolipid-containing liposomes (GLLs) and Siglec-1 expressing CHO cells, the same nine gangliosides were tested by flow cytometry, and binding was observed for GM1, GM2, GD1a, GD1b, GD3 and GT1b, but not for GM3, GM4 and GQ1b.[55] Binding to GM3, however, was detected when the GM3 content was increased to 20 mol %. A liposome over lectin assay, employing Siglec-1 Fc and GLLs containing GM1, GD1a, GD3 and GQ1b detected binding to all four gangliosides. However, the relative binding profile differed from that inferred from the ELISA data.[55] These same four GLLs were also found to bind to Siglec-1 Fc adhered to a streptavidin microbead in a bead assay, with GD1a exhibiting the highest affinity.[55] To explain the variation in binding profiles observed with the different methods, it was proposed that not only affinity but other factors are important for the detection of these interactions, such as steric crowding and the differing presentation of interactions in solution and in a lipid bilayer.[55]

To more firmly establish the ganglioside binding properties of Siglec-1, MEAN-nMS was performed using a DBCO-labeled small monomeric Siglec-1 fragment, consisting of its first three extracellular domains, and the panel of ganglioside-containing NDs described above. Notably, signal corresponding to the 1:1 complex of the membrane anchor-linked Siglec-1 bound to each of the gangliosides was detected (Figures 2c,d, 3c, and S10), with F_{GSL} ranging from 0.5 to 0.8. In contrast, nMS analysis failed to detect any binding between the gangliosides and unlabeled Siglec-1 fragment (Figures 3c and S11). The MEAN-nMS data suggest that all eight of the tested gangliosides are ligands, which is consistent with the reported results obtained with the lipid bilayer-free ELISA.[55] These findings are also in agreement with the ganglioside oligosaccharide affinity data that show Siglec-1 recognizes all eight oligosaccharides, with $GM3_{os}$ being the highest affinity

https://doi.org/10.1021/jacs.4c05805
J. Am. Chem. Soc. XXXX, XXX, XXX−XXX

ligand (Figure S12 and Table S1). To rule out the possibility that any of ganglioside hits result from nonspecific binding, lactosylceramide (LacCer)-containing azidoPE ND was introduced as a negative control. Importantly, no binding to LacCer was observed (Figure 2d), a result in agreement with an absence of detectable binding between the Siglec-1 fragment and lactose disaccharide (Table S1).

To further probe the ganglioside binding properties of Siglec-1, MEAN-CaR-nMS screening of azidoPE-NDs containing a mixture of GSLs extracted from porcine brain against DBCO-labeled Siglec-1 fragment was performed. Chromatographic analysis [hydrophilic interaction liquid chromatography−ultra-high-performance liquid chromatography (HILIC−UHPLC)] of the glycolipid extract identified, in agreement with previous reports,[56] GM1, fucosylated-GM1, GD1a, GT1a, and GT1b as the most abundant GSLs, with GD1b, GD2, GM2, GM3, GQ1, GD3, and GT3 present at lower abundance (Figures S13a and S14a, Table S2). Implementation of the MEAN-CaR-nMS assay identified binding to GM1 and FucGM1, as well as to one or more GD1, FucGD1, and GT1 isomeric species (Figures 4a and S14a). Notably, the observation of binding to FucGM1 and FucGD1, which has not been previously reported, is at odds with the suggestion that the fucosylation of GSLs inhibits Siglec binding.[49]

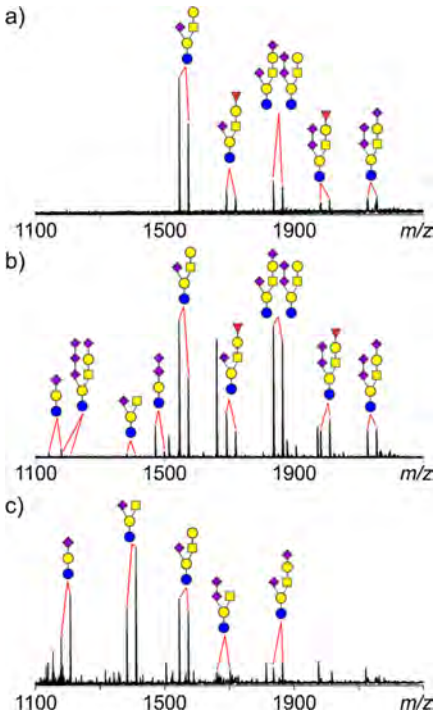

Figure 4. Demonstration of shotgun glycomics screening using MEAN-CaR-nMS and NDs. Results of MEAN-CaR-nMS screening of 20% azidoPE-ND (2 μM) containing a natural library of GSLs from porcine brain against (a) DBCO-labeled Siglec-1 fragment (3 μM), and (b) SARS-CoV-2 RBD (6 μM). (c) Results of MEAN-CaR-nMS screening of a 20% azidoPE-ND containing six GSLs (1% each of GM1, GM2, GM3, GD1a, GD2, and GT1b, each at 10 μM) against DBCO-labeled SARS-CoV-2 RBD (10 μM). All measurements were performed in negative ion mode on aqueous ammonium acetate solutions (200 mM, 25 °C, and pH 6.8). The ceramide moiety was omitted from the GSL structures shown.

SARS-CoV-2 RBD. The spike protein and RBD of SARS-CoV-2 (Wuhan strain) have been shown to recognize diverse acidic and neutral human glycan structures.[57−71] According to the results of nMS-based screening, the oligosaccharides of GM1 and GM2 exhibit the highest affinity of the glycans tested. Numerous other ganglioside oligosaccharides ($GA1_{os}$, $GA2_{os}$, $GD1a_{os}$, $GD1b_{os}$, $GD2_{os}$, $GD3_{os}$, $GM1b_{os}$, $GM3_{os}$, $GT2_{os}$, and $GT3_{os}$) were also found to bind; no binding to $GT1a_{os}$ and $GT1c_{os}$ was detected.[62] To confirm that RBD recognizes gangliosides in a membrane environment, CaR-nMS measurements were performed on NDs containing GM1, GM2, GM3, GD1a, GD2, and GT1b. Binding to GM1, GM2, and GM3 was observed, but no binding was detectable for GT1b, or to GD1a and GD2. Notably, GD1a and GD2 are expected to be ligands based on the oligosaccharide binding data.[62]

To clarify the ganglioside binding properties of SARS-CoV-2 RBD, MEAN-CaR-nMS was used to screen azidoPE-NDs, containing either a mixture of the six gangliosides or porcine brain glycolipid extract, against DBCO-labeled RBD. For the glycolipid extract, binding to GM1, FucGM1, GM2, and GM3, as well as species of GD1, FucGD1, GD2, GQ1, GD3, and GT1 was observed (Figures 4b and S14a). Notably, RBD recognition of FucGD1 has not been previously reported. Importantly, of the six purified gangliosides tested, binding was measured for all except GT1b (Figure 4c), in agreement with the oligosaccharide affinity data.[62]

Together, the screening data acquired for the Siglec-1 fragment and RBD highlight the significant improvements achieved with MEAN-(CaR)-nMS for discovering low-affinity GSL ligands of GBPs. Particularly relevant is that both GBPs possess a single binding site and, therefore, cannot engage in multivalent binding. However, the addition of the membrane anchor enables the detection of low-affinity and, in the case of the glycolipid extract, low abundance ligands. Moreover, these data confirm the promiscuous binding of Siglec-1 to gangliosides and establish that SARS-CoV-2 RBD recognizes a variety of host gangliosides, which could serve as cellular attachment factors for infection.

Application of MEAN-CaR-nMS to Cells. The screening data acquired for the ND sample produced from the porcine brain glycolipid extract demonstrate the feasibility of combining MEAN-CaR-nMS with a shotgun glycomics screening strategy for discovering GSL ligands present in cell membranes. However, glycolipid extraction is inherently biased owing to nonuniform extraction efficiencies and, as a result, ligands with low extraction efficiency may be missed.[72] In contrast, directly measuring GBP binding to GSLs in the cell membrane would avoid extraction biases, albeit with no possibility for enrichment. As of yet, however, GSL ligand discovery through direct cell analysis has not been feasible due to an absence of analytical methods capable of both detecting weak GBP binding to GSLs (in cells) and establishing ligand identity. In principle, nMS analysis can directly detect GBP binding to GSLs on cells but has hitherto lacked the sensitivity needed to detect low-affinity interactions. As described below, the development of MEAN-(CaR)-nMS makes such measurements possible.

To apply MEAN-CaR-nMS to cells, azidoPE must first be incorporated into the cells. While this can, in principle, be achieved through incubation with azidoPE micelles, this route was found to give a low incorporation efficiency, as judged by the absence of membrane anchor formation in experiments

https://doi.org/10.1021/jacs.4c05805
J. Am. Chem. Soc. XXXX, XXX, XXX−XXX

performed using DBCO-labeled GAL-3C (data not shown). Instead, 20% azidoPE-ND was added to a solution containing approximately 5×10^4 cells (at an azidoPE-ND/cell ratio in the 10^8 to 10^9 range) and the mixture was sonicated at room temperature for 30 min. According to optical and scanning electron microscopy images (Figure S15), sonication disrupts the cells resulting in membrane fragments. Therefore, we speculate that it is the fragments that take up azidoPE from the NDs, enabling the formation of the membrane anchor with the labeled GBP. Following an additional 1 h incubation with DBCO-labeled GBP, CaR-nMS analysis was performed.

To demonstrate the capability of MEAN-CaR-nMS to directly detect GSL ligands in cultured cells, measurements were performed to identify ligands of GAL-3C and SARS-CoV-2 RBD in HEK 293T and SH-SY5Y cells. The GSL content of both cell types was assessed by HILIC−UHPLC−MS analysis of the glycolipid extract; CID was employed to confirm the identity of the observed GSLs (Figures S13b,c and S14b,c; Tables S3 and S4). According to this analysis, GM3 (65% of GSLs) and GM2 (22%) are the dominant gangliosides in the HEK 293T cells; GD3, GM1, GD2, GD1a and GD1b are also present but at much lower abundances (3−9%). In the SH-SY5Y cells, GM2 (61% of GSLs) dominates; GD1a is the next most abundant (16%), with GM1, GM3, GD2, GD1b and GT1b also present but at relatively low abundances (4−10%). Screening the azidoPE-treated HEK 293T cells against DBCO-labeled GAL-3C detected the release of GM3, which is the major GSL in the cell membrane (Figure 5a). Only the C18:1/16:0 form of GM3, the most abundant ceramide form in the membrane, was detected. In contrast, no binding was detected by CaR-nMS performed using unlabeled GAL-3C (Figure S16a). Screening these same cells against DBCO-labeled RBD identified both GM3 (C18:1/16:0, C18:1/24:0) and GM2 (C18:1/16:0 and C18:1/18:0) ligands (Figures 5b, S14b, and S17a,b, and Table S3). The three GM3 species represent the most abundant ceramide forms present; the same is true for the two GM2 species detected (Figure S17a,b). No ligand binding was detected from screening performed against the unlabeled RBD (Figure S16b).

In the case of the azidoPE-treated SH-SY5Y neuroblastoma cells, screening against labeled and unlabeled GAL-3C failed to detected any GSL binding (Figures 5c and S16c). These results are consistent with GAL-3C not recognizing GM2, which is the major ganglioside in these cells (Figures S13c and S14c). While no ligands were identified from screening of the unlabeled RBD (Figure S16d), binding to several GM2 species [C18:1/16:0, C18:1/18:0, C18:1/20:0, C18:1/22:0, and C18:1/24:1(15Z)] to labeled RBD was measured (Figures 5d and S17c; Table S4). Curiously though, the relative abundances of released GM2 species do not reflect their relative abundances in the membrane (Figure S17c). For example, despite C18:1/16:0 being present at very low abundance (comprising only ∼0.02% of the identified GM2 species), it represents a significant fraction (∼20%) of the GM2 released from the RBD (Figure S17c). Conversely, the C18:1/22:0 species, which is in high abundance in the cells (∼38%), represents a lower percentage of the released GM2 (17%). These findings raise the possibility that SARS-CoV-2 utilization of host gangliosides as attachment factors is modulated by their ceramide profile. However, this effect remains to be conclusively established.

Although preliminary, these data establish, for the first time, the possibility of directly detecting binding of GBPs to GSL ligands in cultured cells using MEAN-CaR-nMS. That binding was only detected for the most abundant GSLs present indicates a need to improve the sensitivity of the assay. Possible remedies include developing mitigation strategies for the signal suppression that accompanies the use of a larger number of cells in the analysis and alternative delivery routes for enhancing the efficiency of azidoPE incorporation into the cells. Efforts in these directions are ongoing.

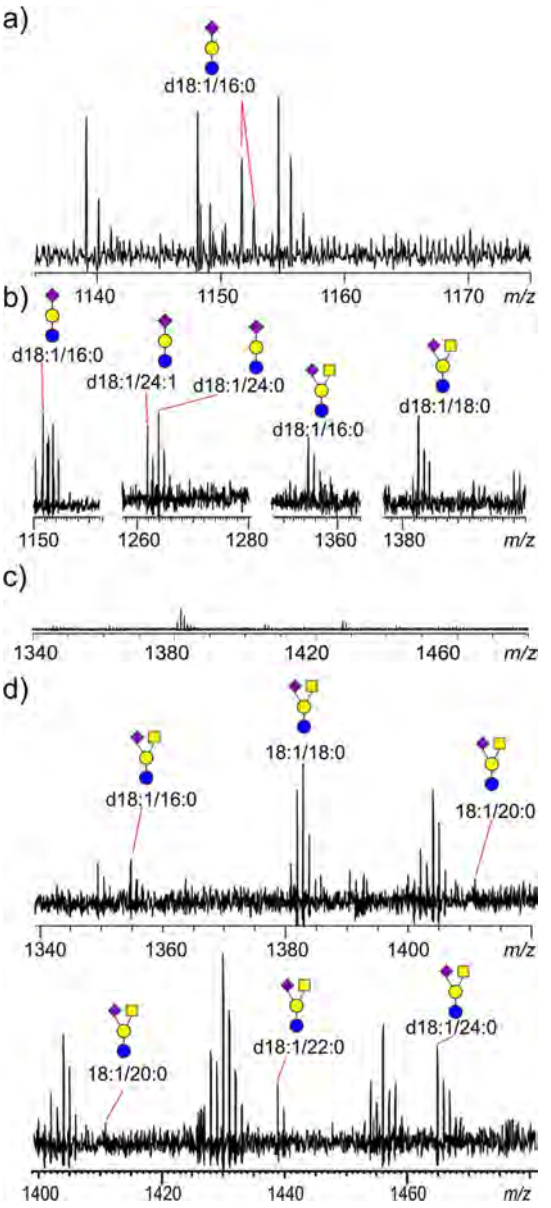

Figure 5. Demonstration of shotgun glycomics screening using MEAN-CaR-nMS and cultured cells. Results of MEAN-CaR-nMS screening of azidoPE-treated HEK 293T cells (5×10^4) against DBCO-labeled (a) GAL-3C (6 μM) and (b) SARS-CoV-2 RBD (6 μM). Results of MEAN-CaR-nMS screening of azidoPE-treated SH-SY5Y neuroblastoma cells (5×10^4) against DBCO-labeled (c) GAL-3C (6 μM) and (d) SARS-CoV-2 RBD (6 μM). The ceramide moiety was omitted from the GSL structures shown.

CONCLUSIONS

This work introduces MEAN-(CaR)-nMS, an innovative assay for detecting low-affinity (K_d ∼mM) interactions between soluble GBPs and GSLs incorporated into model membranes,

https://doi.org/10.1021/jacs.4c05805
J. Am. Chem. Soc. XXXX, XXX, XXX−XXX

such as NDs. The method relies on introducing a membrane anchor to localize the GBP on the surface of the membrane, thereby increasing the effective concentration of GSL in the vicinity of the GBP, which promotes binding. The increase in local GSL concentration, estimated to be as high as 1500 times that of bulk concentration, can produce a >10-fold increase in fractional occupancy of the GBP binding site(s). Importantly, the assay can be implemented with GBPs possessing a single binding site and which cannot engage in multivalent binding as a way to enhance avidity for GSL ligands, as well as multisubunit GBPs. Ligands are identified by detection of intact GBP−GSL complexes (MEAN-nMS) or upon their release from GBP−GSL complexes (MEAN-CaR-nMS).

The results of screening libraries of purified gangliosides incorporated into NDs against immune lectins demonstrate the significant gains in performance achieved through the introduction of the membrane anchor. In the absence of a membrane anchor, nMS analysis yielded predominantly false negatives. In contrast, all ligands were identified by MEAN-(CaR)-nMS, with no false positives. Screening data acquired using NDs produced from natural libraries of GSLs human and viral GBPs showcase the potential of MEAN-CaR-nMS for shotgun glycomics applications to uncover elusive, biologically relevant GSL ligands. Remarkably, MEAN-CaR-nMS allowed, for the first time, nMS-based detection of GBP binding to GSL ligands in cells. While further optimization of the assay for direct analysis of cells is needed, these preliminary data highlight the tremendous potential of nMS, when implemented with a membrane anchor strategy, for discovering GSL ligands and, possibly, other classes of ligands, directly from cell membranes. Uncovering the repertoire of natural GSL ligands of endogenous and exogenous GBPs is essential to a comprehensive understanding of the roles played by GBP−GSL interactions in human health and disease and will help drive the development of new therapeutics and diagnostics.

■ ASSOCIATED CONTENT

Supporting Information

The Supporting Information is available free of charge at https://pubs.acs.org/doi/10.1021/jacs.4c05805.

Additional details about proteins and reagents; cell lines; preparation of NDs; experimental procedures and conditions; data analysis procedures and related equations; summary of affinities; structures of GSLs and click reagents; mass spectra and UHPLC chromatograms (PDF)

■ AUTHOR INFORMATION

Corresponding Author

John S. Klassen − *Department of Chemistry, University of Alberta, Edmonton, Alberta T6G 2G2, Canada;* orcid.org/0000-0002-3389-7112; Phone: (780) 492-3501; Email: john.klassen@ualberta.ca

Authors

James W. Favell − *Department of Chemistry, University of Alberta, Edmonton, Alberta T6G 2G2, Canada*

Duong T. Bui − *Department of Chemistry, University of Alberta, Edmonton, Alberta T6G 2G2, Canada;* orcid.org/0000-0001-9274-0759

Jianing Li − *Department of Chemistry, University of Alberta, Edmonton, Alberta T6G 2G2, Canada*

Ling Han − *Department of Chemistry, University of Alberta, Edmonton, Alberta T6G 2G2, Canada;* orcid.org/0000-0002-3088-0374

Elena N. Kitova − *Department of Chemistry, University of Alberta, Edmonton, Alberta T6G 2G2, Canada*

Edward N. Schmidt − *Department of Chemistry, University of Alberta, Edmonton, Alberta T6G 2G2, Canada*

Raelynn Brassard − *Department of Biochemistry, University of Alberta, Edmonton, Alberta T6G 2H7, Canada*

Pavel I. Kitov − *Department of Chemistry, University of Alberta, Edmonton, Alberta T6G 2G2, Canada*

Yves St-Pierre − *INRS-Institut Armand-Frappier, Laval, Québec H7V 1B7, Canada*

Lara K. Mahal − *Department of Chemistry, University of Alberta, Edmonton, Alberta T6G 2G2, Canada;* orcid.org/0000-0003-4791-8524

M. Joanne Lemieux − *Department of Biochemistry, University of Alberta, Edmonton, Alberta T6G 2H7, Canada;* orcid.org/0000-0003-4745-9153

Matthew S. Macauley − *Department of Chemistry, University of Alberta, Edmonton, Alberta T6G 2G2, Canada; Department of Medical Microbiology and Immunology, University of Alberta, Edmonton, Alberta T6G 2E1, Canada;* orcid.org/0000-0003-4579-1048

Complete contact information is available at: https://pubs.acs.org/10.1021/jacs.4c05805

Notes

The authors declare no competing financial interest.

■ ACKNOWLEDGMENTS

The authors acknowledge funding from the Natural Sciences and Engineering Research Council of Canada (J.S.K., M.S.M., M.J.L.), the Canada Foundation for Innovation (J.S.K., M.J.L.), the Alberta Innovation and Advanced Education Research Capacity Program (J.S.K.), MITACS (R.B.), the Canadian Institutes of Health Research (M.J.L., Y.S.-P.), and the Canada Research Chairs (M.S.M.) and Canada Excellence Research Chairs (L.K.M.) programs. The authors also thank Professors Chris Cairo (University of Alberta) and Stephen M. Tompkins (University of Georgia) for generously providing proteins used in this work.

■ REFERENCES

(1) Daniotti, J. L.; Lardone, R. D.; Vilcaes, A. A. Dysregulated Expression of Glycolipids in Tumor Cells: From Negative Modulator of Anti-Tumor Immunity to Promising Targets for Developing Therapeutic Agents. *Front. Oncol.* **2016**, *5*, 300.

(2) Malhotra, R. Membrane Glycolipids: Functional Heterogeneity: A Review. *Biochem. Anal. Biochem.* **2012**, *1*, 108.

(3) Zuverink, M.; Barbieri, J. T. Protein Toxins That Utilize Gangliosides as Host Receptors. *Prog. Mol. Biol. Transl. Sci.* **2018**, *156*, 325−354.

(4) Ledeen, R. W.; Kopitz, J.; Abad-Rodríguez, J.; Gabius, H. J. Glycan Chains of Gangliosides: Functional Ligands for Tissue Lectins (Siglecs/Galectins). *Prog. Mol. Biol. Transl. Sci.* **2018**, *156*, 289−324.

(5) Zhang, T.; de Waard, A. A.; Wuhrer, M.; Spaapen, R. M. The Role of Glycosphingolipids in Immune Cell Functions. *Front. Immunol.* **2019**, *10*, 90.

(6) Merrill, A. H.; Wang, M. D.; Park, M.; Sullards, M. C. (Glyco)Sphingolipidology: An Amazing Challenge and Opportunity for Systems Biology. *Trends Biochem. Sci.* **2007**, *32*, 457−468.

(7) Cummings, R. D.; Pierce, J. M. The Challenge and Promise of Glycomics. *Chem. Biol.* **2014**, *21*, 1−15.

(8) Cummings, R. D. The Repertoire of Glycan Determinants in the Human Glycome. *Mol. Biosyst.* **2009**, *5*, 1087−1104.
(9) Guo, Z. The Structural Diversity of Natural Glycosphingolipids (GSLs). *J. Carbohydr. Chem.* **2022**, *41*, 63−154.
(10) Avanti Polar Lipids, Inc. https://avantilipids.com/product-category/sphingolipids/glycosphingolipids (accessed Nov 7, 2023).
(11) Leney, A. C.; Fan, X.; Kitova, E. N.; Klassen, J. S. Nanodiscs and Electrospray Ionization Mass Spectrometry: A Tool for Screening Glycolipids against Proteins. *Anal. Chem.* **2014**, *86*, 5271−5277.
(12) Lingwood, C. A.; Manis, A.; Mahfoud, R.; Khan, F.; Binnington, B.; Mylvaganam, M. New Aspects of the Regulation of Glycosphingolipid Receptor Function. *Chem. Phys. Lipids* **2010**, *163*, 27−35.
(13) Han, L.; Nguyen, L.; Schmidt, E. N.; Esmaili, M.; Kitova, E. N.; Overduin, M.; Macauley, M. S.; Klassen, J. S. How Choice of Model Membrane Affects Protein-Glycosphingolipid Interactions: Insights from Native Mass Spectrometry. *Anal. Chem.* **2022**, *94*, 16042−16049.
(14) Rodrigues, E.; Jung, J.; Park, H.; Loo, C.; Soukhtehzari, S.; Kitova, E. N.; Mozaneh, F.; Daskhan, G.; Schmidt, E. N.; Aghanya, V.; Sarkar, S.; Streith, L.; St. Laurent, C. D.; Nguyen, L.; Julien, J. P.; West, L. J.; Williams, K. C.; Klassen, J. S.; Macauley, M. S. A Versatile Soluble Siglec Scaffold for Sensitive and Quantitative Detection of Glycan Ligands. *Nat. Commun.* **2020**, *11*, 5091.
(15) MacKenzie, C. R.; Hirama, T. Quantitative Analyses of Binding Affinity and Specificity for Glycolipid Receptors by Surface Plasmon Resonance. *Methods Enzymol.* **2000**, *312*, 205−216.
(16) Berselli, G. B.; Sarangi, N. K.; Gimenez, A. V.; Murphy, P. V.; Keyes, T. E. Microcavity Array Supported Lipid Bilayer Models of Ganglioside - Influenza Hemagglutinin1binding. *Chem. Commun.* **2020**, *56*, 11251−11254.
(17) Castellana, E. T.; Cremer, P. S. Solid Supported Lipid Bilayers: From Biophysical Studies to Sensor Design. *Surf. Sci. Rep.* **2006**, *61*, 429−444.
(18) Worstell, N. C.; Krishnan, P.; Weatherston, J. D.; Wu, H. J. Binding Cooperativity Matters: A Gm1-like Ganglioside-Cholera Toxin b Subunit Binding Study Using a Nanocube-Based Lipid Bilayer Array. *PLoS One* **2016**, *11*, No. e0153265.
(19) Worstell, N. C.; Singla, A.; Saenkham, P.; Galbadage, T.; Sule, P.; Lee, D.; Mohr, A.; Kwon, J. S. I.; Cirillo, J. D.; Wu, H. J. Hetero-Multivalency of Pseudomonas Aeruginosa Lectin LecA Binding to Model Membranes. *Sci. Rep.* **2018**, *8*, 8419.
(20) Saliba, A. E.; Vonkova, I.; Gavin, A. C. The Systematic Analysis of Protein-Lipid Interactions Comes of Age. *Nat. Rev. Mol. Cell Biol.* **2015**, *16*, 753−761.
(21) Grant, O. C.; Smith, H. M. K.; Firsova, D.; Fadda, E.; Woods, R. J. Presentation, Presentation, Presentation! Molecular-Level Insight into Linker Effects on Glycan Array Screening Data. *Glycobiology* **2014**, *24*, 17−25.
(22) Han, L.; Kitov, P. I.; Li, J.; Kitova, E. N.; Klassen, J. S. Probing Heteromultivalent Protein-Glycosphingolipid Interactions Using Native Mass Spectrometry and Nanodiscs. *Anal. Chem.* **2020**, *92*, 3923−3931.
(23) Kitova, E. N.; El-Hawiet, A.; Schnier, P. D.; Klassen, J. S. Reliable Determinations of Protein-Ligand Interactions by Direct ESI-MS Measurements. Are We There Yet? *J. Am. Soc. Mass Spectrom.* **2012**, *23*, 431−441.
(24) Wang, W.; Kitova, E. N.; Klassen, J. S. Influence of Solution and Gas Phase Processes on Protein-Carbohydrate Binding Affinities Determined by Nanoelectrospray Fourier Transform Ion Cyclotron Resonance Mass Spectrometry. *Anal. Chem.* **2003**, *75*, 4945−4955.
(25) Zhang, Y.; Liu, L.; Daneshfar, R.; Kitova, E. N.; Li, C.; Jia, F.; Cairo, C. W.; Klassen, J. S. Protein-Glycosphingolipid Interactions Revealed Using Catch-and-Release Mass Spectrometry. *Anal. Chem.* **2012**, *84*, 7618−7621.
(26) Leney, A. C.; Rezaei Darestani, R.; Li, J.; Nikjah, S.; Kitova, E. N.; Zou, C.; Cairo, C. W.; Xiong, Z. J.; Privé, G. G.; Klassen, J. S. Picodiscs for Facile Protein-Glycolipid Interaction Analysis. *Anal. Chem.* **2015**, *87*, 4402−4408.
(27) Li, J.; Fan, X.; Kitova, E. N.; Zou, C.; Cairo, C. W.; Eugenio, L.; Ng, K. K. S.; Xiong, Z. J.; Privé, G. G.; Klassen, J. S. Screening Glycolipids Against Proteins in Vitro Using Picodiscs and Catch-and-Release Electrospray Ionization-Mass Spectrometry. *Anal. Chem.* **2016**, *88*, 4742−4750.
(28) Li, J.; Richards, M. R.; Bagal, D.; Campuzano, I. D. G.; Kitova, E. N.; Xiong, Z. J.; Privé, G. G.; Klassen, J. S. Characterizing the Size and Composition of Saposin A Lipoprotein Picodiscs. *Anal. Chem.* **2016**, *88*, 9524−9531.
(29) Li, J.; Han, L.; Li, J.; Kitova, E. N.; Xiong, Z. J.; Privé, G. G.; Klassen, J. S. Detecting Protein-Glycolipid Interactions Using CaR-ESI-MS and Model Membranes: Comparison of Pre-Loaded and Passively Loaded Picodiscs. *J. Am. Soc. Mass Spectrom.* **2018**, *29*, 1493−1504.
(30) Cohen, M.; Varki, A. Modulation of Glycan Recognition by Clustered Saccharide Patches. *Int. Rev. Cell Mol. Biol.* **2014**, *308*, 75−125.
(31) El-Hawiet, A.; Kitova, E. N.; Klassen, J. S. Quantifying Carbohydrate-Protein Interactions by Electrospray Ionization Mass Spectrometry Analysis. *Biochemistry* **2012**, *51*, 4244−4253.
(32) Báez Bolivar, E. G.; Bui, D. T.; Kitova, E. N.; Han, L.; Zheng, R. B.; Luber, E. J.; Sayed, S. Y.; Mahal, L. K.; Klassen, J. S. Submicron Emitters Enable Reliable Quantification of Weak Protein-Glycan Interactions by ESI-MS. *Anal. Chem.* **2021**, *93*, 4231−4239.
(33) Han, L.; Morales, L. C.; Richards, M. R.; Kitova, E. N.; Sipione, S.; Klassen, J. S. Investigating the Influence of Membrane Composition on Protein-Glycolipid Binding Using Nanodiscs and Proxy Ligand Electrospray Ionization Mass Spectrometry. *Anal. Chem.* **2017**, *89* (17), 9330−9338.
(34) Overduin, M.; Esmaili, M. Native Nanodiscs and the Convergence of Lipidomics, Metabolomics, Interactomics and Proteomics. *Appl. Sci.* **2019**, *9*, 1230.
(35) North, S. J.; Jang-Lee, J.; Harrison, R.; Canis, K.; Ismail, M. N.; Trollope, A.; Antonopoulos, A.; Pang, P. C.; Grassi, P.; Al-Chalabi, S.; Etienne, A. T.; Dell, A.; Haslam, S. M. Mass Spectrometric Analysis of Mutant Mice. *Methods Enzymol.* **2010**, *478*, 27−77.
(36) Yoon, H. Y.; Lee, D.; Lim, D. K.; Koo, H.; Kim, K. Copper-Free Click Chemistry: Applications in Drug Delivery, Cell Tracking, and Tissue Engineering. *Adv. Mater.* **2022**, *34*, 2107192.
(37) Ruan, Q.; Zhao, C. A Method for Parallel Microscale Protein Labeling and Precise Control over the Average Degree of Labeling (ADoL). *Sci. Rep.* **2023**, *13*, 8961.
(38) Vira, S.; Mekhedov, E.; Humphrey, G.; Blank, P. S. Fluorescent-Labeled Antibodies: Balancing Functionality and Degree of Labeling. *Anal. Biochem.* **2010**, *402*, 146−150.
(39) Han, L.; Kitova, E. N.; Li, J.; Nikjah, S.; Lin, H.; Pluvinage, B.; Boraston, A. B.; Klassen, J. S. Protein-Glycolipid Interactions Studied in Vitro Using ESI-MS and Nanodiscs: Insights into the Mechanisms and Energetics of Binding. *Anal. Chem.* **2015**, *87*, 4888−4896.
(40) Varki, A.; Cummings, R. D.; Esko, J. D.; Stanley, P.; Hart, G. W.; Aebi, M.; Darvill, A. G.; Kinoshita, T.; Packer, N. H.; Prestegard, J. H.; Schnaar, R. L.; Seeberg, P. H. *Essentials of Glycobiology*, 4th ed.; Cold Spring Harbor Laboratory Press: Cold Spring Harbor, NY, 2022.
(41) Collins, P. M.; Bum-Erdene, K.; Yu, X.; Blanchard, H. Galectin-3 Interactions with Glycosphingolipids. *J. Mol. Biol.* **2014**, *426*, 1439−1451.
(42) Nehmé, R.; St-Pierre, Y. Targeting Intracellular Galectins for Cancer Treatment. *Front. Immunol.* **2023**, *14*, 1269391.
(43) St-Pierre, Y.; Campion, C. G.; Grosset, A. A. A Distinctive Role for Galectin-7 in Cancer? *Front. Biosci.* **2012**, *17*, 438−450.
(44) Vander Zanden, C. M.; Majewski, J.; Weissbarth, Y.; Browne, D. F.; Watkins, E. B.; Gabius, H. J. Structure of Galectin-3 Bound to a Model Membrane Containing Ganglioside GM1. *Biophys. J.* **2023**, *122*, 1926−1937.
(45) Kopitz, J.; André, S.; Von Reitzenstein, C.; Versluis, K.; Kaltner, H.; Pieters, R. J.; Wasano, K.; Kuwabara, I.; Liu, F. T.; Cantz, M.; Heck, A. J. R.; Gabius, H. J. Homodimeric Galectin-7 (P53-Induced

https://doi.org/10.1021/jacs.4c05805
J. Am. Chem. Soc. XXXX, XXX, XXX−XXX

Gene 1) Is a Negative Growth Regulator for Human Neuroblastoma Cells. *Oncogene* **2003**, *22*, 6277−6288.
(46) Shams-Ud-Doha, K.; Kitova, E. N.; Kitov, P. I.; St-Pierre, Y.; Klassen, J. S. Human Milk Oligosaccharide Specificities of Human Galectins. Comparison of Electrospray Ionization Mass Spectrometry and Glycan Microarray Screening Results. *Anal. Chem.* **2017**, *89*, 4914−4921.
(47) Morris, S.; Ahmad, N.; Andre, S.; Kaltner, H.; Gabius, H. J.; Brenowitz, M.; Brewer, F. Quaternary Solution Structures of Galectins-1, −3, and −7. *Glycobiology* **2004**, *14*, 293−300.
(48) Siuda, I.; Tieleman, D. P. Molecular Models of Nanodiscs. *J. Chem. Theory Comput.* **2015**, *11*, 4923−4932.
(49) Varki, A.; Angata, T. Siglecs - The Major Subfamily of I-Type Lectins. *Glycobiology* **2006**, *16*, 1−27.
(50) Prenzler, S.; Rudrawar, S.; Waespy, M.; Kelm, S.; Anoopkumar-Dukie, S.; Haselhorst, T. The Role of Sialic Acid-Binding Immunoglobulin-like-Lectin-1 (Siglec-1) in Immunology and Infectious Disease. *Int. Rev. Immunol.* **2023**, *42*, 113−138.
(51) Crocker, P. R.; Paulson, J. C.; Varki, A. Siglecs and Their Roles in the Immune System. *Nat. Rev. Immunol.* **2007**, *7*, 255−266.
(52) Macauley, M. S.; Crocker, P. R.; Paulson, J. C. Siglec-Mediated Regulation of Immune Cell Function in Disease. *Nat. Rev. Immunol.* **2014**, *14*, 653−666.
(53) Schnaar, R. L. Gangliosides as Siglec Ligands. *Glycoconj. J.* **2023**, *40*, 159−167.
(54) Eakin, A. J.; Bustard, M. J.; Mcgeough, C. M.; Ahmed, T.; Bjourson, A. J.; Gibson, D. S. Siglec-1 and −2 as Potential Biomarkers in Autoimmune Disease. *Proteomics: Clin. Appl.* **2016**, *10*, 635−644.
(55) Schmidt, E. N.; Lamprinaki, D.; McCord, K. A.; Joe, M.; Sojitra, M.; Waldow, A.; Nguyen, J.; Monyror, J.; Kitova, E. N.; Mozaneh, F.; Guo, X. Y.; Jung, J.; Enterina, J. R.; Daskhan, G. C.; Han, L.; Krysler, A. R.; Cromwell, C. R.; Hubbard, B. P.; West, L. J.; Kulka, M.; Sipione, S.; Klassen, J. S.; Derda, R.; Lowary, T. L.; Mahal, L. K.; Riddell, M. R.; Macauley, M. S. Siglec-6 Mediates the Uptake of Extracellular Vesicles through a Noncanonical Glycolipid Binding Pocket. *Nat. Commun.* **2023**, *14*, 2327.
(56) Hájek, R.; Jirásko, R.; Lísa, M.; Cífková, E.; Holčapek, M. Hydrophilic Interaction Liquid Chromatography-Mass Spectrometry Characterization of Gangliosides in Biological Samples. *Anal. Chem.* **2017**, *89*, 12425−12432.
(57) Tortorici, M. A.; Walls, A. C.; Lang, Y.; Wang, C.; Li, Z.; Koerhuis, D.; Boons, G. J.; Bosch, B. J.; Rey, F. A.; de Groot, R. J.; Veesler, D. Structural Basis for Human Coronavirus Attachment to Sialic Acid Receptors. *Nat. Struct. Mol. Biol.* **2019**, *26*, 481−489.
(58) Yang, Y.; Du, Y.; Kaltashov, I. A. The Utility of Native MS for Understanding the Mechanism of Action of Repurposed Therapeutics in COVID-19: Heparin as a Disruptor of the SARS-COV-2 Interaction with Its Host Cell Receptor. *Anal. Chem.* **2020**, *92*, 10930−10934.
(59) Oh, L.; Varki, A.; Chen, X.; Wang, L. P. SARS-CoV-2 and MERS-CoV Spike Protein Binding Studies Support Stable Mimic of Bound 9-O-Acetylated Sialic Acids. *Molecules* **2022**, *27*, 5322.
(60) Tomris, I.; Unione, L.; Nguyen, L.; Zaree, P.; Bouwman, K. M.; Liu, L.; Li, Z.; Fok, J. A.; Ríos Carrasco, M.; van der Woude, R.; Kimpel, A. L. M.; Linthorst, M. W.; Kilavuzoglu, S. E.; Verpalen, E. C. J. M.; Caniels, T. G.; Sanders, R. W.; Heesters, B. A.; Pieters, R. J.; Jiménez-Barbero, J.; Klassen, J. S.; Boons, G. J.; de Vries, R. P. SARS-CoV-2 Spike N-Terminal Domain Engages 9-*O*-Acetylated α2−8-Linked Sialic Acids. *ACS Chem. Biol.* **2023**, *18*, 1180−1191.
(61) Petitjean, S. J. L.; Chen, W.; Koehler, M.; Jimmidi, R.; Yang, J.; Mohammed, D.; Juniku, B.; Stanifer, M. L.; Boulant, S.; Vincent, S. P.; Alsteens, D. Multivalent 9-O-Acetylated-Sialic Acid Glycoclusters as Potent Inhibitors for SARS-CoV-2 Infection. *Nat. Commun.* **2022**, *13*, 2564.
(62) Nguyen, L.; McCord, K. A.; Bui, D. T.; Bouwman, K. M.; Kitova, E. N.; Elaish, M.; Kumawat, D.; Daskhan, G. C.; Tomris, I.; Han, L.; Chopra, P.; Yang, T. J.; Willows, S. D.; Mason, A. L.; Mahal, L. K.; Lowary, T. L.; West, L. J.; Hsu, S. T. D.; Hobman, T.; Tompkins, S. M.; Boons, G. J.; de Vries, R. P.; Macauley, M. S.; Klassen, J. S. Sialic Acid-Containing Glycolipids Mediate Binding and Viral Entry of SARS-CoV-2. *Nat. Chem. Biol.* **2022**, *18*, 81−90.
(63) Baker, A. N.; Richards, S. J.; Guy, C. S.; Congdon, T. R.; Hasan, M.; Zwetsloot, A. J.; Gallo, A.; Lewandowski, J. R.; Stansfeld, P. J.; Straube, A.; Walker, M.; Chessa, S.; Pergolizzi, G.; Dedola, S.; Field, R. A.; Gibson, M. I. The SARS-COV-2 Spike Protein Binds Sialic Acids and Enables Rapid Detection in a Lateral Flow Point of Care Diagnostic Device. *ACS Cent. Sci.* **2020**, *6*, 2046−2052.
(64) Liu, L.; Chopra, P.; Li, X.; Bouwman, K. M.; Tompkins, S. M.; Wolfert, M. A.; De Vries, R. P.; Boons, G. J. Heparan Sulfate Proteoglycans as Attachment Factor for SARS-CoV-2. *ACS Cent. Sci.* **2021**, *7*, 1009−1018.
(65) Guimond, S. E.; Mycroft-West, C. J.; Gandhi, N. S.; Tree, J. A.; Le, T. T.; Spalluto, C. M.; Humbert, M. V.; Buttigieg, K. R.; Coombes, N.; Elmore, M. J.; Wand, M.; Nyström, K.; Said, J.; Setoh, Y. X.; Amarilla, A. A.; Modhiran, N.; Sng, J. D. J.; Chhabra, M.; Young, P. R.; Rawle, D. J.; Lima, M. A.; Yates, E. A.; Karlsson, R.; Miller, R. L.; Chen, Y. H.; Bagdonaite, I.; Yang, Z.; Stewart, J.; Nguyen, D.; Laidlaw, S.; Hammond, E.; Dredge, K.; Wilkinson, T. M. A.; Watterson, D.; Khromykh, A. A.; Suhrbier, A.; Carroll, M. W.; Trybala, E.; Bergström, T.; Ferro, V.; Skidmore, M. A.; Turnbull, J. E. Synthetic Heparan Sulfate Mimetic Pixatimod (PG545) Potently Inhibits SARS-CoV-2 by Disrupting the Spike-ACE2 Interaction. *ACS Cent. Sci.* **2022**, *8*, 527−545.
(66) Ryzhikov, A. B.; Onkhonova, G. S.; Imatdinov, I. R.; Gavrilova, E. V.; Maksyutov, R. A.; Gordeeva, E. A.; Pazynina, G. V.; Ryzhov, I. M.; Shilova, N. V.; Bovin, N. V. Recombinant SARS-CoV-2 S Protein Binds to Glycans of the Lactosamine Family in Vitro. *Biochemistry* **2021**, *86*, 243−247.
(67) Dhar, C.; Sasmal, A.; Diaz, S.; Verhagen, A.; Yu, H.; Li, W.; Chen, X.; Varki, A. Are Sialic Acids Involved in COVID-19 Pathogenesis? *Glycobiology* **2021**, *31*, 1068−1071.
(68) Wu, S. C.; Arthur, C. M.; Wang, J.; Verkerke, H.; Josephson, C. D.; Kalman, D.; Roback, J. D.; Cummings, R. D.; Stowell, S. R. The SARS-CoV-2 Receptor-Binding Domain Preferentially Recognizes Blood Group A. *Blood Adv.* **2021**, *5*, 1305−1309.
(69) Yang, Q.; Hughes, T. A.; Kelkar, A.; Yu, X.; Cheng, K.; Park, S. J.; Huang, W. C.; Lovell, J. F.; Neelamegham, S. Inhibition of SARS-CoV-2 Viral Entry upon Blocking N-and O-Glycan Elaboration. *Elife* **2020**, *9*, No. e61552.
(70) Saso, W.; Yamasaki, M.; Nakakita, S. I.; Fukushi, S.; Tsuchimoto, K.; Watanabe, N.; Sriwilaijaroen, N.; Kanie, O.; Muramatsu, M.; Takahashi, Y.; Matano, T.; Takeda, M.; Suzuki, Y.; Watashi, K. Significant Role of Host Sialylated Glycans in the Infection and Spread of Severe Acute Respiratory Syndrome Coronavirus 2. *PLoS Pathog.* **2022**, *18*, No. e1010590.
(71) Bui, D. T.; Favell, J.; Kitova, E. N.; Li, Z.; McCord, K. A.; Schmidt, E. N.; Mozaneh, F.; Elaish, M.; El-Hawiet, A.; St-Pierre, Y.; Hobman, T. C.; Macauley, M. S.; Mahal, L. K.; Flynn, M. R.; Klassen, J. S. Absolute Affinities from Quantitative Shotgun Glycomics Using Concentration-Independent (COIN) Native Mass Spectrometry. *ACS Cent. Sci.* **2023**, *9*, 1374−1387.
(72) Aldana, J.; Romero-Otero, A.; Cala, M. P. Exploring the Lipidome: Current Lipid Extraction Techniques for Mass Spectrometry Analysis. *Metabolites* **2020**, *10*, 231.

https://doi.org/10.1021/jacs.4c05805
J. Am. Chem. Soc. XXXX, XXX, XXX−XXX